ARTICLE

ACS chemical biology

Role of Hmbox1 in Endothelial Differentiation of Bone-Marrow Stromal Cells by a Small Molecule

Le Su[†,‡,∥], HongLing Zhao[†,‡,∥], ChunHui Sun[†,‡], BaoXiang Zhao[§,*], Jing Zhao[†,‡], ShangLi Zhang[†,‡], Hua Su[†,‡], and JunYing Miao[†,‡,*]

[†]Institute of Developmental Biology, School of Life Science, Shandong University, Jinan 250100, China, [‡]The Key Laboratory of Cardiovascular Remodeling and Function Research, Chinese Ministry of Education and Chinese Ministry of Health, Shandong University, Qilu Hospital, Jinan 250012, China, and [§]Institute of Organic Chemistry, School of Chemistry and Chemical Engineering, Shandong University, Jinan 250100, China, [∥]These authors contributed equally to this work.

ABSTRACT Bone marrow stromal cells (BMSCs) play critical roles in repairing endothelium damage. However, the mechanisms underlying BMSC differentiation into vascular endothelial cells (VECs) is not well understood. We aimed to find new factors involved in this process by exploiting a novel chemical inducer in a gene microarray assay. We first identified a novel benzoxazine derivative (6-amino-2,3-dihydro-3-hydroxymethyl-1,4-benzoxazine; ABO) that can induce BMSC differentiation to VECs in a capillary-like tube formation assay, promote analysis of endothelial cell-specific marker expression, and facilitate uptake of 1,1′-dioctadecyl-3,3,3′,3′-tetramethylindocarbocyanine perchlorate-acetylated low-density lipoprotein (Dil-Ac-LDL). Microarray analysis of BMSCs treated with ABO for 4 h revealed changes in only a handful of genes. The only one upregulated was homeobox-containing 1 (Hmbox1) gene, whereas six genes, including IP-10 and others, were downregulated. The upregulation of Hmbox1 and downregulation of IP-10 were confirmed by RT-PCR, quantitative PCR (qPCR), and Western blot analysis. It is reported that IP-10 could suppresse EC differentiation into capillary structures. In this study ABO could not induce BMSC differentiation to VECs in the presence of IP-10. Small interfering RNA knockdown of Hmbox1 blocked ABO-induced BMSC differentiation and increased the level of IP-10 but decreased Ets-1. Thus, ABO is a novel inducer for BMSC differentiation to VECs, and Hmbox1 is a key factor in the differentiation. IP-10 and Ets-1 might be relevant targets of Hmbox1 in BMSC differentiation to VECs. These findings provide information on a novel target and a new platform for further investigating the gene control of BMSC differentiation to VECs.

Bone marrow stromal cells (BMSCs) can differentiate into various kinds of cells, including endothelial cells (ECs), osteocytes, chondrocytes, adipocytes, and neural cells. Because BMSCs have low immunogenicity and multilineage differentiation potential, they could be used for generating new tissue and repairing damaged tissue. BMSCs differentiate into ECs, resulting in increased vascularity and improved cardiac function in an ischemia model (*1*). It has been shown that BMSCs differentiate into vascular endothelial cells (VECs) following BMSCs implanted into vein grafting in rats (*2*). These BMSCs cells contribute to rapid re-endothelialization and inhibited neointimal formation and advanced vascular lesion formation (*2*). Differentiation of BMSCs to VECs has been utilized for myocardial regeneration and neoangiogenesis. However, the mechanisms underlying BMSC differentiation to VECs are not well-known.

VECs have been defined by their capacity to interact with small molecules instead of growth factors (*3*). Our previous studies have reported that 6-amino-2,3-dihydro-3-hydroxymethyl-1,4-benzoxazine (ABO) inhibits VEC apoptosis induced by growth factor deprivation and oxidized low-density lipoprotein (*4, 5*). However, the role of ABO in BMSCs differentiation into VECs is not known yet. In this study, we found that ABO is an inducer for BMSC differentiation into VECs. To determine which genes might be involved in this process, we compared gene expression pattern in undifferentiated BMSCs (without ABO treatment) and differentiated BMSCs (with ABO treatment). Using the 27K Rat Genome Array consisting of 28,800 genes of various functional classes, we found that one gene, Hmbox1, was up-regulated, whereas 6 genes were down-regulated.

*Corresponding author, miaojy@sdu.edu.cn.

Received for review November 9, 2009 and accepted September 7, 2010.

Published online September 7, 2010

10.1021/cb100153r

Homeobox genes, essential genes in the genetic control of development, were first identified in Drosophila (*6*). They are characterized by the presence of a DNA sequence, the homeobox, which encodes a protein domain termed the homeodomain. Homeobox domains bind to certain regions of DNA and regulate the transcription of many other genes, several of which in turn play a key role in the control of embryogenesis and cell differentiation, and several have been implicated in human diseases and congenital abnormalities (*7*). Recently, 235 human homeobox genes have been classified into 11 groups on the basis of several criteria, including sequence identity, sequence similarity in the flanking regions, organization into gene clusters, association with other sequence motifs, and position of introns (*8*). Hmbox1 was first identified and isolated from the human pancreatic cDNA library. Human Hmbox1 is composed of 10 exons, spanning about 160 kb at the boundary of chromosomal bands 8p12 and 8p21.1. The open reading frame of human Hmbox1 is 1,263 bp and encodes a putative protein with 421 amino acid residues. It contains a homeobox domain between amino acids 267 and 344 (*9*). However, the role of Hmbox1, a potential transcription repressor, in BMSC differentiation to VECs is unknown.

Interferon-γ-inducible protein 10 (IP-10) is an inhibitor of angiogenesis *in vivo* and suppresses EC differentiation into capillary structures *in vitro* (*10*). IP-10 significantly inhibits vascular endothelial growth factor (VEGF)-induced endothelial motility and tube formation and induces the dissociation of newly formed blood vessels (*11, 12*). Interestingly, gene microarray analysis showed that IP-10 was decreased during the differentiation, suggesting the possible role of IP-10 in this process. To determine the mechanism by which Hmobox1 regulates BMSC differentiation into VECs, we investigated the relationship between Hmbox1 and IP-10 by suppression of Hmbox1.

Ets1, a transcription factor, regulates the expression of genes involved in endothelial function and angiogenesis (*13*). It has been reported that a trans-factor binding site for Ets1 (p54) is upstream of Hmbox1 (*9*). However, the relationship between these 2 transcription factors during BMSC differentiation to VECs is not clear. To answer this question, we investigated the effect of knockdown of Hmbox1 on the expression of Ets1.

RESULTS AND DISCUSSION

ABO Induces BMSC Differentiation to Functional VECs. To investigate the induction effect of ABO on endothelial differentiation of BMSCs, we performed a capillary-like tube formation assay with Matrigel, commonly used for identification of functional VECs *in vitro*. Cells were seeded on Matrigel-coated 24-well plates. Cells treated with 25−100 μM ABO migrated and showed a capillary-like appearance, whereas cells in the control group showed only a dispersed pattern (Figure 1, panels a and b). We also examined the expression of the endothelial-specific markers Flk-1, antihemophiliac factor (AHF), and endothelial nitric oxide synthase (eNOS) by immunofluorescence. As shown in Figure 1, panels c and d, the expression levels of Flk-1, AHF, and eNOS were significantly increased in BMSCs in the presence of ABO compared in the absence of ABO. Since VECs are functionally defined by their capacity to take up DiI-Ac-LDL from plasma (*14*), we found that ABO increased the number of DiI-Ac-LDL-positive VECs (Figure 1, panel e). In terms of the number of positive cells taking up DiI-Ac-LDL, the proportion of BMSCs that differentiated to VECs was 53.74% or 82.13% after treatment with ABO for 24 or 48 h, respectively (Figure 1, panel f). Therefore, ABO promotes BMSC differentiation into functional VECs.

Microarray Analysis in BMSCs Treated with ABO. To determine new molecules that contribute to differentiation of BMSCs to VECs, we analyzed ABO-induced changes in the BMSC gene expression profile by using the 27K Rat Genome Array, which consist of 28,800 genes. We observed that 7 genes have more than 2-fold changes in BMSCs treated with 25 μM ABO for 4 h, including 1 gene up-regulated and 6 genes down-regulated (Figure 2, panels a and b). We confirmed the microarray results by RT-PCR and qPCR and found that Hmbox1 was increased and IP-10 was decreased significantly (Figure 2, panels c−e). To further confirm the gene changes in protein levels of Hmbox1 and IP-10 in ABO-induced differentiation of BMSCs, Hmbox1 showed a 1.6-fold increase and IP-10 a 2.5-fold decrease in protein levels determined by Western blot (Figure 2, panels f and g). Microarray analysis showed the expression of Mx1, ISG15, ADAP1, TRRAP, and PPP1R2 down-regulated during the differentiation, indicating that they might be involved in ABO-induced BMSCs differentiation.

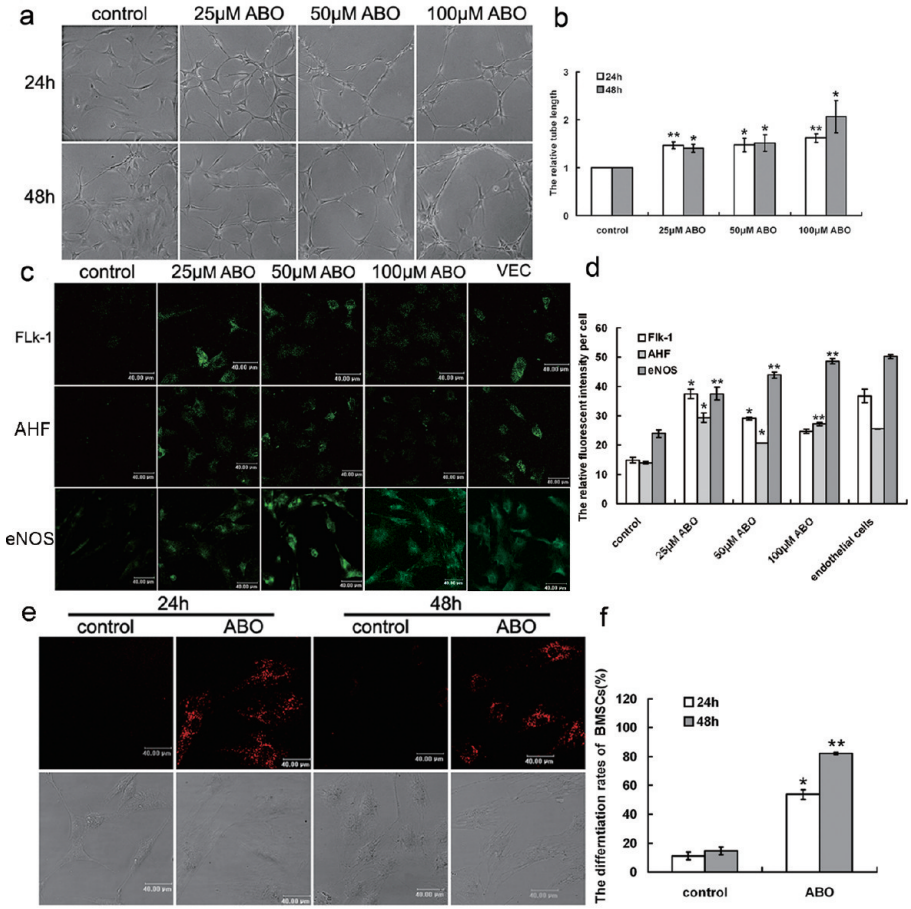

Figure 1. 6-Amino-2,3-dihydro-3-hydroxymethyl-1,4-benzoxazine (ABO) induces bone marrow stromal cell (BMSC) differentiation to functional vascular endothelial cells (VECs). a) ABO promotes vascular structure formation. b) Quantitative assessment of tube formation. (c) Fluorescent intensity of Flk-1, antihemophiliac factor (AHF), and endothelial nitric oxide synthase (eNOS) at 48 h. VEC: human umbilical vascular endothelial cells as a positive control. d) Quantification of relative fluorescence intensity per cell. (* $p < 0.05$, ** $p < 0.01$ *vs* control, $n = 5$). e) Uptake of 1,1′-dioctadecyl-3,3,3′,3′-tetramethylindocarbocyanine perchlorate-acetylated low-density lipoprotein (DiI-Ac-LDL) by cells treated with 50 μM ABO. The gray images are the photographs from the transmission microscopy. f) Differentiation rate of BMSCs.

Knockdown of Hmbox1 Blocks ABO-Induced Differentiation of BMSCs. Hmbox1 was abundantly expressed in pancreas, moderately in brain, placenta, prostate, thymus, and testes (*9*). It has been demonstrated that Hmbox1 is located in both cytoplasm and nuclei of HEK-293T cells and serves as a transcription repressor (*15*). Recently, a splicing variant of Hmbox1, designated Hmbox1b, was found to have the same subcellular localization as Hmbox1 (*16*). To the best of our knowledge, there are no reports about the detailed functions and mechanisms of Hmbox1.

To investigate the role of Hmbox1 in the differentiation of BMSCs to VECs, we inhibited the endogenous expression of Hmbox1 by small interfering RNA (siRNA). Immunofluorescence staining and Western blot analysis showed that 40 nm siRNA effectively inhibited the expression of Hmbox1 at 48 h, and the transfection efficiency was up to 52.63% (Figure 3).

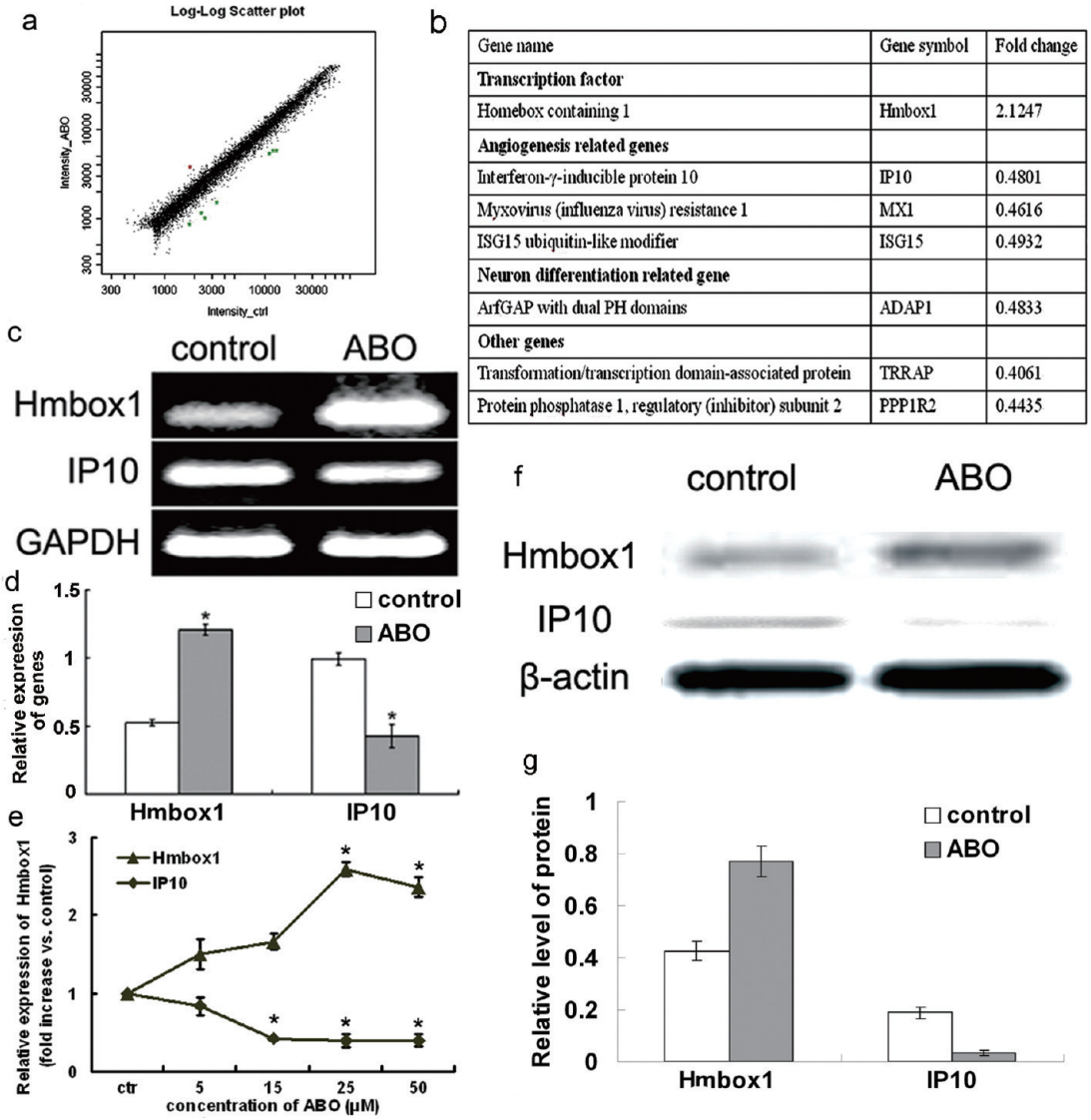

Gene name	Gene symbol	Fold change
Transcription factor		
Homebox containing 1	Hmbox1	2.1247
Angiogenesis related genes		
Interferon-γ-inducible protein 10	IP10	0.4801
Myxovirus (influenza virus) resistance 1	MX1	0.4616
ISG15 ubiquitin-like modifier	ISG15	0.4932
Neuron differentiation related gene		
ArfGAP with dual PH domains	ADAP1	0.4833
Other genes		
Transformation/transcription domain-associated protein	TRRAP	0.4061
Protein phosphatase 1, regulatory (inhibitor) subunit 2	PPP1R2	0.4435

Figure 2. Microarray analysis of gene expression induced by ABO. a) Scatter plot results of gene expression. Red point shows an up-regulated gene; green points show down-regulated genes. b) The 7 genes with more than 2-fold change in expression on microarray analysis. c) RT-PCR results of the expression of Hmbox1 and IP-10 in cells treated with 25 μM ABO for 4 h. GAPDH was used as a normalization control. d) The relative mRNA level of Hmbox1 and IP-10. e) The mRNA level of Hmbox1 and IP-10 by qPCR. f) Western blot analysis of cells treated with 25 μM ABO for 4 h. g) The relative quantity of the proteins shown in panel e. β-actin was used as a normalization control (* $p < 0.05$ *vs* control, $n = 3$).

When Hmbox1 was downregulated, ABO could not increase the levels of Flk-1 and AHF (Figure 4, panels a and b). Moreover, ABO increased the uptake of DiI-Ac-LDL, and this uptake was attenuated when endogenous Hmbox1 was suppressed. Inhibition of Hmbox1 by siRNA decreased the differentiation rate of BMSCs to 21.48% compared with control siRNA (Figure 4, panels c and d). Collectively, our data demonstrate that Hmbox1plays a critical role in ABO-induced differentiation of BMSCs to VECs.

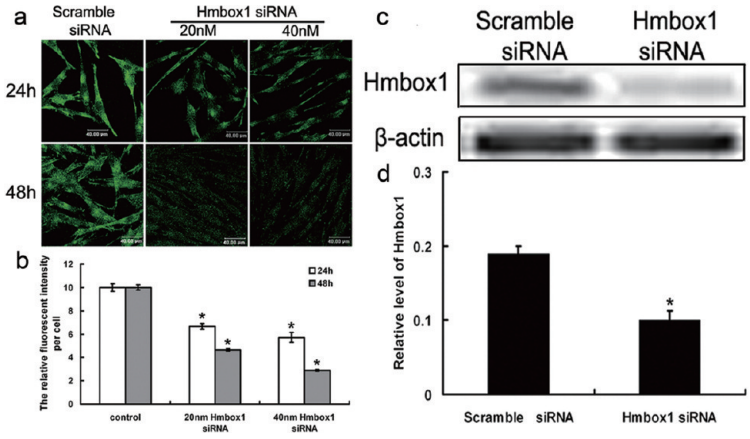

Figure 3. Expression of Hmbox1 is downregulated by small interfering RNA (siRNA). a) siRNA-mediated downregulation of Hmbox1 in BMSCs detected by immunofluorescence assay. b) The relative quantity of Hmbox1 shown in panel a. Scramble siRNA: cells transfected with scramble control siRNA, 40 nM. Hmbox1 siRNA: cells transfected with Hmbox1 siRNA (* $p < 0.05$ *vs* control, $n = 3$). c) Western blot analysis of Hmbox1 protein level. Protein extracts were from cells treated with siRNA or scramble control siRNA, 40 nM, for 48 h. d) Relative quantity of Hmbox1 protein level shown in panel c (* $p < 0.05$ *vs* control, $n = 3$).

Hmbox1 Regulates IP-10 and Ets-1 Expression. Since the binding site for Ets1 (p54) exists in the region 1,000 bp upstream of Hmbox1 (*9*), Ets1 might be regulated by Hmbox1. However, whether Hmbox1 affects Ets1 expression is not known. We found that knockdown of Hmbox1 *via* siRNA decreased the levels of Ets-1, while the level of IP-10 was elevated (Figure 5, panels a and b). Thus, Hmbox1 may promote the differentiation of BMSCs to VECs by regulating the expression of IP-10 and Ets-1.

IP-10 Decreases VEC Differentiation from BMSCs Induced by ABO. IP-10, chemokine (C-X-C motif) ligand 10 (CXCL10), a member of the α chemokine family, inhibits bone marrow colony formation and has antitumor activity *in vivo*. It is a chemoattractant for human monocytes and T cells and promotes T-cell adhesion to endothelial cells (*17–19*). IP-10 inhibits angiogenesis *in vivo* and suppress endothelial cell differentiation into capillary structures *in vitro*. IP-10 significantly inhibits VEGF-induced endothelial motility and tube formation (*11*). A recent report showed that IP-10 induces dissociation of newly formed blood vessels (*12*). However, whether IP-10 is implicated in differentiation of BMSCs to VECs is not known.

We have shown that the expression of IP-10 was decreased in the presence of VEC differentiation from BMSCs (Figure 2). To define whether IP-10 prevents the differentiation of BMSCs, we treated BMSCs with ABO in the presence of IP-10. The results showed that the increased uptake of DiI-Ac-LDL induced by ABO was inhibited by IP-10 and the differentiation rate of BMSCs decreased to 47.56% in the presence of ABO and IP-10 compared with the cells

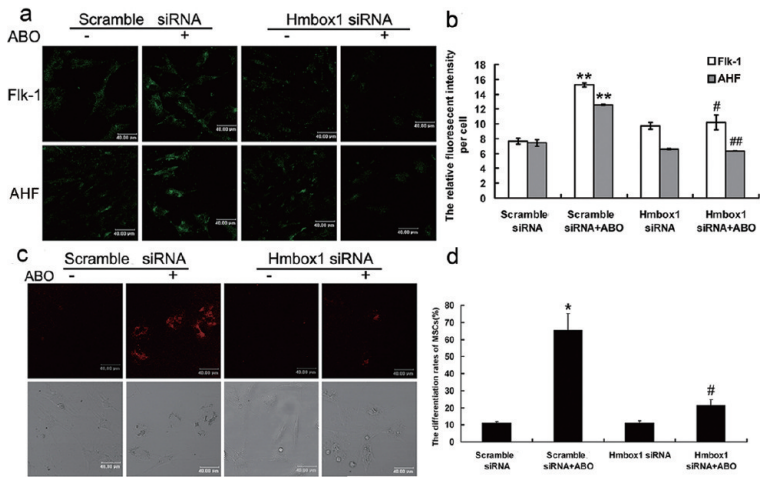

Figure 4. Knockdown of Hmbox1 blocks ABO-induced differentiation of BMSCs. a) Levels of Flk-1 and AHF analyzed by immunofluorescence assay at 48 h. b) Quantification of relative fluorescence intensity per cell of the scan shown in panel a) ($p < 0.01$ *vs* #, ** $p < 0.01$ *vs* ##, $n = 3$). c) The uptake of DiI-Ac-LDL by cells. Scramble siRNA + ABO: cells treated with scramble siRNA and ABO; Hmbox1 siRNA + ABO: cells treated with Hmbox1 siRNA and ABO. The gray images are the photographs from the transmission microscopy. d) Differentiation rate of BMSCs (* $p < 0.05$ *vs* #, $n = 3$).**

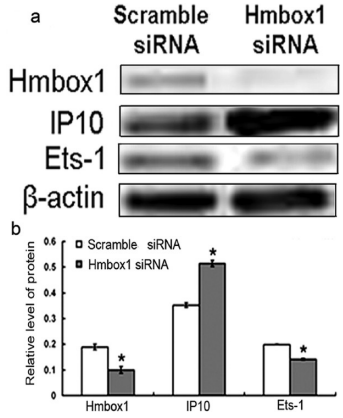

Figure 5. Hmbox1 modulates the expression of IP-10 and Ets-1. a) Western blot analysis of cells treated with Hmbox1 siRNA or scramble control siRNA, 40 nM, for 48 h. b) The relative quantity of proteins shown in panel a (* $p < 0.05$ *vs* control, $n = 3$).

treated with ABO alone (Figure 6, panels a and b), suggesting that IP-10 prevents VEC differentiation from BMSCs. We found that knockdown of Hmobox1 increased the expression of IP-10. Although Hmbox1 is a potential transcription repressor, which genes are suppressed by Hmbox1 is not clear. Here, we provide the evidence that IP-10 may be a target regulated by Hmbox1 during BMSC differentiation to VECs.

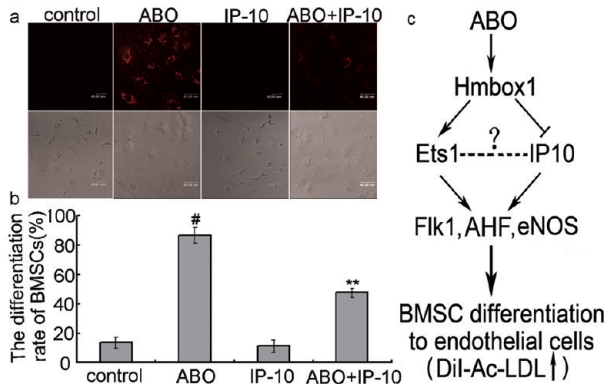

Figure 6. IP-10 prevents VEC differentiation from BMSCs. a) The uptake of DiI-Ac-LDL by the cells in control, ABO, IP-10, and ABO + IP-10 groups. The gray images are the photographs from the transmission microscopy. b) The differentiation rate ($p < 0.05$ *vs* #, $n = 3$). c) Working model of BMSC differentiation to VECs induced by ABO. ABO targets Hmbox1. Then, Hmbox1 downregulates IP-10 and upregulates Ets-1, which induces BMSC differentiation to VECs *via* elevation of the levels of Flk-1, AHF, and eNOS accompanied by increased DiI-Ac-LDL uptake.**

Recent evidence revealed that Ets1 is required for VEC survival during embryonic angiogenesis, while VEC apoptosis was significantly increased when Ets1 was mutated (*20*). In terms of the relatively specific expression pattern of Ets1 in embryo VECs, a VEC-specific element for expression of Ets1 was identified in the first intron of Ets1 gene (*21*). The role of Ets family members during angiogenesis has been partly addressed by the dissection of the cis-acting elements involved in the regulation of endothelial-specific genes, including Tie, VE-cadherin, Flk-1, and eNOS (*22*–*25*). In this study, differentiation of BMSCs to VECs induced by ABO elevated levels of Ets1, along with increased expression of endothelial-specific genes such as Flk1, AHF, and eNOS. Thus, we presumed that the transcription repressor Hmbox1 downregulated IP-10 and upregulated Ets1, resulting in increased levels of endothelial-specific genes and inducing the differentiation (Figure 6, panel c).

IP-10 and Ets1 have a similar DNA rearrangement that could effectively maintain homeostatic control and contribute to the neoplastic state (*26*). Here, we found that both IP-10 and Ets1 could be regulated by Hmbox1 in the differentiation of BMSCs to VECs, which indicates that IP-10 and Ets1 might work together in this process (Figure 6, panel c), although the detailed relationship between the 2 genes needs further investigation.

In our previous study, we synthesized a series of 2,3-dihydro-3-hydroxymethyl-1,4-benzoxazine derivatives by tandem reduction-oxirane opening of 2-nitroaroxymethyloxiranes (Supplementary Figure 1). Among the 7 compounds (**3a**−**g**), only ABO (**3g**) markedly inhibited the apoptosis of human umbilical cord endothelial cells (*4*). Moreover, we found that ABO induced angiogenesis both *in vitro* and *in vivo* (*27*). Therefore, we investigated the role of ABO in inducing BMSC differentiation to VECs. From the structures of the 7 compounds, only ABO possesses an amino group at the 6-position. Therefore, we speculated that the amino group at the 6-position of ABO might be important for its action, although the particular working model of ABO needs to be investigated.

In summary, our experiments with the inducer ABO provide compelling evidence that the transcription repressor Hmbox1 can regulate the differentiation of BMSCs to VECs by suppressing the expression of IP-10 and

increasing that of Ets1. The data suggest that ABO is a useful tool for understanding the mechanism of BMSC differentiation to VECs. Hmbox1 is a key factor involved in the differentiation. IP-10 and Ets-1 might be the relevant targets of Hmbox1 in this process. The findings of this work provide a novel target for BMSC differentiation to VECs for further investigation into the functions of Hmbox1.

METHODS

Cell Culture. Rat BMSCs were isolated from the femurs and tibias of male Wistar rats (90−100 g) as described earlier with modification (*28*). Briefly, the cells were seeded in Dulbecco's modified Eagle's medium low glucose (Gibco, USA) supplemented with 20% fetal bovine serum (FBS; Hyclone, USA) and fibroblast growth factor 2 (FGF-2), 5 ng mL^{-1}, at 37 °C in humidified air with 5% CO_2. Rat BMSCs were phenotypically characterized as described (*29*). When BMSCs reached subconfluence, cells were washed twice with the medium and separated into 2 groups for treatment: incubated in basal medium (without FBS and FGF-2) but with dimethyl sulfoxide (DMSO) <0.1% (v/v) or in basal medium (without FBS and FGF-2) with 25, 50, or 100 μM ABO. Fresh ABO was dissolved in DMSO and applied to cells for a final concentration of DMSO < 0.1% (v/v) in the culture medium. DMSO at 0.1% (v/v) did not affect cell viability. The cells in the 2 treatment groups were incubated for 4, 6, 8, 12, 24, or 48 h.

***In Vitro* Capillary-Like Tube Formation Assay.** The formation of vascular-like structures in BMSCs was assessed by use of growth-factor-reduced Matrigel (BD Biosciences, USA) as previously described (*30*). BMSCs were seeded on 24-well plates coated with Matrigel at $4-5 \times 10^4$ cells per well in basal DMEM medium and incubated at 37 °C for 60 min. Cells were treated with or without ABO small molecule in the absence of FGF-2 and serum and then incubated at 37 °C for 48 h. Tube formation was observed by use of an inverted-phase contrast microscope (Nikon, Japan) at 24 and 48 h. The degree of tube formation was quantified by measuring the length of tubes in random fields from each well by use of the National Institutes of Health Image program.

Immunofluorescence Assay. Immunofluorescence assay was performed as described (*31*). After adding the primary antibodies (rabbit anti-rat Flk-1, AHF, eNOS, or Hmbox1 IgG) and appropriate secondary antibodies (fluorescein isothiocyanate [FITC]-goat anti-rabbit IgG; all Biotechnology, Santa Cruz, CA), the samples were evaluated by laser scanning confocal microscopy (LSCM) (Leica, Germany). Targeted proteins displayed green fluorescence after excitation at 488 nm. We randomly selected the region of interest and then zoomed in the same frames. The relative fluorescent intensity per cell was the total value of the sample in the zoom scan divided by the total number of cells (at least 200 cells) in the same scan.

Dil-Ac-LDL Uptake Assay. BMSCs were seeded on 24-well culture plates. Subconfluent cultured cells were washed twice with basal medium and then treated as described above for 24 or 48 h. Then, cells were incubated in 10 μg mL^{-1} 1,1′-dioctadecyl-3,3,3′,3′-tetramethylindocarbocyanine perchlorate-acetylated low-density lipoprotein (Dil-Ac-LDL) (Invitrogen, USA) at 37 °C for 4 to 6 h. The media was removed and cells were washed once with the culture media. The cells that could uptake Dil-Ac-LDL showed red fluorescence with LSCM excitation at 543 nm. The ability to uptake Dil-Ac-LDL was used to estimate the differentiation rate of BMSCs: the number of positively stained cells divided by the total number of cells in random visual fields. At least 200 cells for each sample were counted.

Microarray Analysis. Total RNA was extracted from cells treated with DMSO alone or 25 μM ABO for 4 h with TRIzol reagent (Invitrogen, USA). The samples were stored at −20 °C, and microarray analysis was performed by CapitalBio Corp. (http://www.capitalbio.com). The microarray experimental procedures were as described (*32*).

Semiquantitative RT-PCR and Quantitative Real-Time PCR (qPCR). Semiquantitative RT-PCR analysis of BMSCs treated as described above for Hmbox1 and IP-10 genes was as described (*31*). Briefly, total RNA was isolated from cells with use of TRIzol reagent, and 2 μg of RNA was reverse-transcribed with use of M-MLV reverse transcriptase (Promega, USA) according to the manufacturer's instructions. The specific primers were for Hmbox1, sense 5′-GTC CAG GAG GCC ATT CCA ACA GCG-3′, antisense 5′-AAT GAG GGC ACC ATG CCA TCT TC-3′; IP-10, sense 5′-CAT TCC TGC AAG TCT ATC CTG T-3′, antisense 5′-GGA GAG ACC GTC TCT CTG CT-3′; and GAPDH (as a normalization control), sense 5′-TAT CGG ACG CCT GGT TAC-3′, antisense 5′-TGA GCC CTT CCA TAT GC-3′.

The qPCR reactions involved use of the ABI 7000 PCR System (Applied Biosystems, Germany) with SYBR Green PCR Master Mix (Applied Biosystems). Samples were analyzed in triplicate. The level of each gene was calculated by comparing the Ct value in the samples to a standard curve generated from serially diluted cDNA from a reference sample and normalization to the level of GAPDH. The primer sequences of the genes of interest are given above.

Transient Transfection and RNA Interference. To knock down the expression of Hmbox1 protein, RNA interference (RNAi) was performed as described (*33*). Specific siRNA against Hmbox1 was designed and synthesized by Invitrogen (USA). The synthesized siRNA to Hmbox1 was (RNA)-UUU CAG AGA CGU AAC UCG UUC CAG G (sense) and (RNA)-CCU GGA ACG AGU UAC GUC UCU GAA A (antisense). BMSCs at 50−60% confluence were transfected with Hmbox1 siRNA (20−40 nM) by use of RNAiFect Transfection Reagent according to the manufacturer's instructions (QIAGEN, Germany). We monitored the effect of gene silencing by immunofluorescence staining at 24−48 h after transfection and Western blot analysis. Scramble siRNA was used as a control (Santa Cruz Biotechnology, USA).

Western Blot Analysis. Western blot was performed as described previously (*34*). Briefly, the cells were lysed in protein lysis buffer containing 25 mM Tris-HCl (pH 6.8), 2% SDS, 6% glycerol, 1% 2-mercaptoethanol, 2 mM PMSF, 0.2‰ bromphenol blue, and a protease inhibitor cocktail (Sigma, St. Louis, MO) for 10 min at RT and boiled for another 10 min. The protein concentration was determined by Coomassie brilliant blue protein assay. The cellular proteins (30 μg) were applied to 12% SDS-polyacrylamide gel and electroblotted onto polyvinylidene difluoride (PVDF) membrane. The membrane was blocked with 5% (w/v) nonfat dry milk in phosphate buffered saline (PBS)-Tween 20 (PBST; 0.05%) for 1 h and incubated with anti-Hmbox1, anti-Ets-1, anti-IP-10 or anti-β-actin antibody (Santa Cruz, Biotechnology) at 4 °C overnight. After a washing in PBST and PBS, the PVDF membrane was incubated with appropriate horseradish peroxidase-conjugated secondary antibodies (Santa Cruz, Biotechnology) for 1 h at RT. The immunoreactive bands were chromogenously developed with use of 3,3′-diaminobenzidine. β-Actin was used as a loading control. The

relative quantity of proteins was analyzed by use of Quantity One software (Bio-Rad, USA).

IP-10 Prevents VEC Differentiation from BMSCs. Cells were divided into four groups. In the control group, cells were incubated in the basal medium. In the ABO treatment group, cells were incubated in the basal medium with 25 μM ABO for 48 h. In the IP-10 group, cells were treated with IP-10 (R&D Systems) 200 ng mL^{-1} for 48 h (*35*). In the ABO + IP-10 group, cells were treated with ABO and IP-10 together for 48 h. Then the cells were incubated in 10 μg mL^{-1} Dil-Ac-LDL (Invitrogen, USA) at 37 °C for 4−6 h. The medium was then removed, and the cells were washed once with the culture medium. The samples were evaluated at the 543 nm (wavelength) under the laser scanning confocal microscope (Leica, Germany). The ability to uptake Dil-Ac-LDL was used to estimate the differentiation rate of BMSCs. The differentiation rate of BMSCs equaled to the number of positively stained cells divided by the total number of cells in random visual fields. At least 200 cells for each sample were counted.

Statistical Analyses. Data are expressed as mean ± SE. SPSS v11.5 (SPSS Inc., Chicago, IL) was used for statistical analysis. Comparisons among groups involved one-way ANOVA followed by Scheffé F-test posthoc analysis. A $P < 0.05$ was considered statistically significant.

Acknowledgment: This study was supported in part by the National Natural Science Foundation of China (No.90813022 and 81021001), the National 973 Research Project (No. 2011CB503900), the Science and Technology Development Project of Shandong Province (2008GG10002034 and Z2008D04), and the Independent Innovation Foundation of Shandong University (2009JC007, 2009GN033).

Supporting Information Available: This material is available free of charge *via* the Internet at http://pubs.acs.org.

REFERENCES

1. Silva, G.-V., Litovsky, S., Assad, J.-A., Sousa, A.-L., Martin, B.-J., Vela, D., Coulter, S.-C., Lin, J., Ober, J., Vaughn, W.-K., Branco, R.-V., Oliveira, E.-M., He, R., Geng, Y.-J., Willerson, J.-T., and Perin, E.-C. (2005) Mesenchymal stem cells differentiate into an endothelial phenotype, enhance vascular density, and improve heart function in a canine chronic ischemia model, *Circulation 111*, 150−156.
2. Yue, W.-M., Liu, W., Bi, Y.-W., He, X.-P., Sun, W.-Y., Pang, X.-Y., Gu, X.-H., and Wang, X.-P. (2008) Mesenchymal stem cells differentiate into an endothelial phenotype, reduce neointimal formation, and enhance endothelial function in a rat vein grafting model, *Stem Cells Dev. 17*, 785−793.
3. Chen, S., Borowiak, M., Fox, J.-L., Maehr, R., Osafune, K., Davidow, L., Lam, K., Peng, L.-F., Schreiber, S.-L., Rubin, L.-L., and Melton, D. (2009) A small molecule that directs differentiation of human ESCs into the pancreatic lineage, *Nat. Chem. Biol. 5*, 258−265.
4. Jiao, P.-F., Zhao, B.-X., Wang, W.-W., He, Q.-X., Wan, M.-S., Shin, D.-S., and Miao, J.-Y. (2006) Design, synthesis, and preliminary biological evaluation of 2,3-dihydro-3-hydroxymethyl-1,4-benzoxazine derivatives, *Bioorg. Med. Chem. Lett. 16*, 2862−2867.
5. Liu, X., Zhao, J., Xu, J., Zhao, B., Zhang, Y., Zhang, S., and Miao, J. (2009) Protective effects of a benzoxazine derivative against oxidized LDL-induced apoptosis and the increases of integrin beta4, ROS, NF-kappaB and P53 in human umbilical vein endothelial cells, *Bioorg. Med. Chem. Lett. 19*, 2896−2900.
6. Lawrence, P.-A., and Morata, G. (1994) Homeobox genes: their function in Drosophila segmentation and pattern formation, *Cell 78*, 181−189.
7. Levine, M., and Hoey, T. (1988) Homeobox proteins as sequence-specific transcription factors, *Cell 55*, 537−540.
8. Holland, P.-W., Booth, H.-A., and Bruford, E.-A. (2007) Classification and nomenclature of all human homeobox genes, *BMC Biol. 5*, 47.
9. Chen, S., Saiyin, H., Zeng, X., Xi, J., Liu, X., Li, X., and Yu, L. (2006) Isolation and functional analysis of human HMBOX1, a homeobox containing protein with transcriptional repressor activity, *Cytogenet. Genome Res. 114*, 131−136.
10. Angiolillo, A.-L., Sgadari, C., Taub, D.-D., Liao, F., Farber, J.-M., Maheshwari, S., Kleinman, H.-K., Reaman, G.-H., and Tosato, G. (1995) Human interferon-inducible protein 10 is a potent inhibitor of angiogenesis in vivo, *J. Exp. Med. 182*, 155−162.
11. Bodnar, R.-J., Yates, C.-C., and Wells, A. (2006) IP-10 blocks vascular endothelial growth factor-induced endothelial cell motility and tube formation via inhibition of calpain, *Circ. Res. 98*, 617−625.
12. Bodnar, R.-J., Yates, C.-C., Rodgers, M.-E., Du, X., and Wells, A. (2009) IP-10 induces dissociation of newly formed blood vessels, *J. Cell Sci. 122*, 2064−2077.
13. Lelievre, E., Lionneton, F., Soncin, F., and Vandenbunder, B. (2001) The Ets family contains transcriptional activators and repressors involved in angiogenesis, *Int. J. Biochem. Cell Biol. 33*, 391−407.
14. Voyta, J.-C., Via, D.-P., Butterfield, C.-E., and Zetter, B.-R. (1984) Identification and isolation of endothelial cells based on their increased uptake of acetylated-low density lipoprotein, *J. Cell Biol. 99*, 2034−2040.
15. Dai, J., Wu, L., Zhang, C., Zheng, X., Tian, Z., and Zhang, J. (2009) Recombinant expression of a novel human transcriptional repressor HMBOX1 and preparation of anti-HMBOX1 monoclonal antibody, *Cell Mol. Immunol. 6*, 261−268.
16. Zhang, M., Chen, S., Li, Q., Ling, Y., Zhang, J., and Yu, L. (2009) Characterization of a novel human HMBOX1 splicing variant lacking the homeodomain and with attenuated transcription repressor activity, *Mol. Biol. Rep. 37*, 2767−2772.
17. Luster, A.-D., and Leder, P. (1993) IP-10, a -C-X-C- chemokine, elicits a potent thymus-dependent antitumor response in vivo, *J. Exp. Med. 178*, 1057−1065.
18. Taub, D.-D., Lloyd, A.-R., Conlon, K., Wang, J.-M., Ortaldo, J.-R., Harada, A., Matsushima, K., Kelvin, D.-J., and Oppenheim, J.-J. (1993) Recombinant human interferon-inducible protein 10 is a chemoattractant for human monocytes and T lymphocytes and promotes T cell adhesion to endothelial cells, *J. Exp. Med. 177*, 1809−1814.
19. Sarris, A.-H., Broxmeyer, H.-E., Wirthmueller, U., Karasavvas, N., Cooper, S., Lu, L., Krueger, J., and Ravetch, J.-V. (1993) Human interferon-inducible protein 10: expression and purification of recombinant protein demonstrate inhibition of early human hematopoietic progenitors, *J. Exp. Med. 178*, 1127−1132.
20. Wei, G., Srinivasan, R., Cantemir-Stone, C.-Z., Sharma, S.-M., Santhanam, R., Weinstein, M., Muthusamy, N., Man, A.-K., Oshima, R.-G., Leone, G, and Ostrowski, M.-C. (2009) Ets1 and Ets2 are required for endothelial cell survival during embryonic angiogenesis, *Blood 114*, 1123−1130.
21. Jorcyk, C.-L., Garrett, L.-J., Maroulakou, I.-G., Watson, D.-K., and Green, J.-E. (1997) Multiple regulatory regions control the expression of Ets-1 in the developing mouse: vascular expression conferred by intron I, *Cell Mol. Biol. 43*, 211−225.
22. Iljin, K., Dube, A., Kontusaari, S., Korhonen, J., Lahtinen, I., Oettgen, P., and Alitalo, K. (1999) Role of ets factors in the activity and endothelial cell specificity of the mouse Tie gene promoter, *FASEB J. 13*, 377−386.
23. Lelievre, E., Mattot, V., Huber, P., Vandenbunder, B., and Soncin, F. (2000) ETS1 lowers capillary endothelial cell density at confluence and induces the expression of VE-cadherin, *Oncogene 19*, 2438−2446.
24. Kappel, A., Schlaeger, T.-M., Flamme, I., Orkin, S.-H., Risau, W., and Breier, G. (2000) Role of SCL/Tal-1, GATA, and ets transcription factor binding sites for the regulation of flk-1 expression during murine vascular development, *Blood 96*, 3078−3085.

25. Karantzoulis-Fegaras, F., Antoniou, H., Lai, S.-L., Kulkarni, G., D'Abreo, C., Wong, G.-K., Miller, T.-L., Chan, Y., Atkins, J., Wang, Y., and Marsden, P.-A. (1999) Characterization of the human endothelial nitric-oxide synthase promoter, *J. Biol. Chem. 274*, 3076–3093.
26. Luster, A.-D., Jhanwar, S.-C., Chaganti, R.-S., Kersey, J.-H., and Ravetch, J.-V. (1987) Interferon-inducible gene maps to a chromosomal band associated with a (4;11) translocation in acute leukemia cells, *Proc. Natl. Acad. Sci. U.S.A. 84*, 2868–2871.
27. Dong, Z., Cheng, Y., Zhao, J., Su, L., Zhao, B., Zhang, Y., Zhang, S., and Miao, J. (2010) Discovery of a benzoxazine derivative promoting angiogenesis in vitro and in vivo, *J. Cell Physiol. 223*, 202–208.
28. Pittenger, M.-F., Mackay, A.-M., Beck, S.-C., Jaiswal, R.-K., Douglas, R., Mosca, J.-D., Moorman, M.-A., Simonetti, D.-W., Craig, S., and Marshak, D.-R. (1999) Multilineage potential of adult human mesenchymal stem cells, *Science 284*, 143–147.
29. Wang, N., Xie, K., Huo, S., Zhao, J., Zhang, S., and Miao, J. (2007) Suppressing phosphatidylcholine-specific phospholipase C and elevating ROS level, NADPH oxidase activity and Rb level induced neuronal differentiation in mesenchymal stem cells, *J. Cell Biochem. 100*, 1548–1557.
30. Kureishi, Y., Luo, Z., Shiojima, I., Bialik, A., Fulton, D., Lefer, D.-J., Sessa, W.-C., and Walsh, K. (2000) The HMG-CoA reductase inhibitor simvastatin activates the protein kinase Akt and promotes angiogenesis in normocholesterolemic animals, *Nat. Med. 6*, 1004–1010.
31. Wang, N., Sun, C., Huo, S., Zhang, Y., Zhao, J., Zhang, S., and Miao, J. (2008) Cooperation of phosphatidylcholine-specific phospholipase C and basic fibroblast growth factor in the neural differentiation of mesenchymal stem cells in vitro, *Int. J. Biochem. Cell Biol. 40*, 294–306.
32. Patterson, T.-A., Lobenhofer, E.-K., Fulmer-Smentek, S.-B., Collins, P.-J., Chu, T.-M., Bao, W., Fang, H., Kawasaki, E.-S., Hager, J., Tikhonova, I.-R., Walker, S.-J., Zhang, L., Hurban, P., de Longueville, F., Fuscoe, J.-C., Tong, W., Shi, L., and Wolfinger, R.-D. (2006) Performance comparison of one-color and two-color platforms within the MicroArray Quality Control (MAQC) project, *Nat. Biotechnol. 24*, 1140–1150.
33. Lv, X., Su, L., Yin, D., Sun, C., Zhao, J., Zhang, S., and Miao, J. (2008) Knockdown of integrin beta4 in primary cultured mouse neurons blocks survival and induces apoptosis by elevating NADPH oxidase activity and reactive oxygen species level, *Int. J. Biochem. Cell Biol. 40*, 689–699.
34. Du, A.-Y., Zhao, B.-X., Yin, D.-L., Zhang, S.-L., and Miao, J.-Y. (2005) Discovery of a novel small molecule, 1-ethoxy-3-(3,4-methylenedioxyphenyl)-2-propanol, that induces apoptosis in A549 human lung cancer cells, *Bioorg. Med. Chem. 13*, 4176–4183.
35. Bodnar, R.-J., Yates, C.-C., and Wells, A. (2006) IP-10 blocks vascular endothelial growth factor-induced endothelial cell motility and tube formation via inhibition of calpain, *Circ. Res. 98*, 617–625.